JOC The Journal of Organic Chemistry

Article

pubs.acs.org/joc

Meta–*Para*-Linked Octaaza[1_8]cyclophanes and Their Polycationic States

Daisuke Sakamaki,[†] Akihiro Ito,*[,†] Ko Furukawa,[‡,⊥] Tatsuhisa Kato,[§] and Kazuyoshi Tanaka[†]

[†]Department of Molecular Engineering, Graduate School of Engineering, Kyoto University, Nishikyo-ku, Kyoto 615-8510, Japan

[‡]Institute for Molecular Science, Myodaiji, Okazaki 444-8585, Japan

[§]Institute for the Promotion of Excellence in Higher Education, Kyoto University, Yoshida-Nihonmatsu, Sakyo-ku, Kyoto 606-8501, Japan

Supporting Information

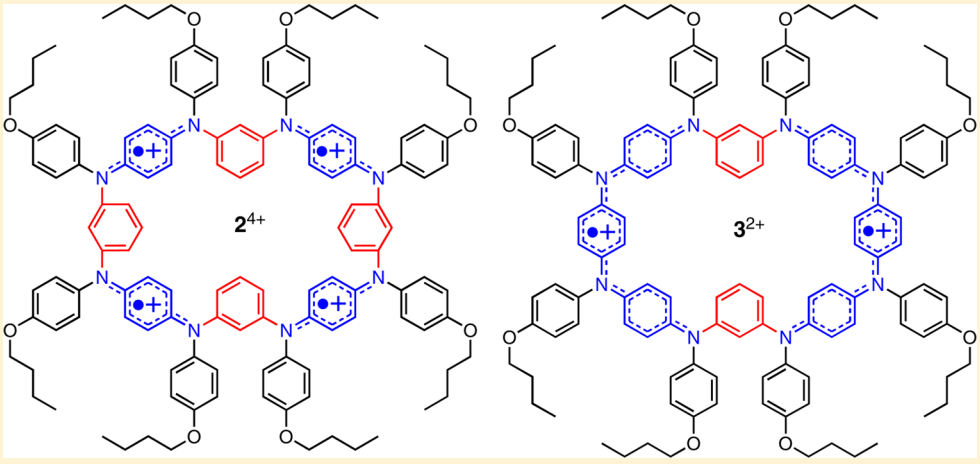

ABSTRACT: Octaazacyclophanes, octaaza[1_8]*m*,*p*,*m*,*p*,*m*,*p*,*m*,*p*-cyclophane (**2**) and octaaza[1_8]*m*,*p*,*p*,*p*,*m*,*p*,*p*,*p*-cyclophane (**3**), as ring-size extended congeners of tetraaza[1_4]*m*,*p*,*m*,*p*-cyclophane were synthesized, and the electronic states of their polycationic species were investigated by quantum chemical calculations, electrochemical measurements (cyclic voltammetry (CV) and differential pulse voltammetry (DPV)), UV–vis–NIR spectroelectrochemical measurements, and pulsed electron spin resonance (ESR) spectroscopy. These octaazacyclophanes exhibited multiredox activities depending on different linkage patterns along the macrocyclic molecular skeletons, and both molecules were oxidizable up to their respective octacations. Spectroelectrochemical measurements demonstrated that *p*-phenylenediamine (PD) moieties in **2** could be converted from the semiquinoidal structure to the quinoidal sturcture with increasing oxidation number, whereas higher oxidation states of **3** did not show definite quinoidal deformation of PD moieties. A pulsed ESR spectrum gave evidence about formation of the almost pure spin-triplet state for $\mathbf{3}^{2+}$, whereas the high-spin states of $\mathbf{2}^{2+}$ and $\mathbf{2}^{4+}$ are virtually degenerate with the competing low-spin states even at low temperatures, probably due to the fragility of spin-coupling pathway caused by facile conformational changes.

INTRODUCTION

Hetera[1_n]cyclophanes, in which the methylene linkages between the arene rings are replaced by heteroatoms, have recently gained considerable interest in conjunction with applications to supramolecular and materials chemistry.[1−4] In particular, the chemistry of aza[1_n]cyclophanes[3−12] has developed rapidly in parallel with their synthetic availability by recent exploitation of palladium-catalyzed aryl amination reactions ("Buchwald–Hartwig reactions"[13]). In addition, aza[1_n]cyclophanes are considered as attractive scaffolds from which multispin systems can be realized,[4] mainly due to their multiredox activity and their stability of generated polycationic species. However, it has been confirmed that strong Coulombic interactions between charged centers generated in aza[1_n]-metacyclophanes prevent the formation of higher oxidation states with high-spin multiplicities (Coulombic penalty).[7,8,14] As we have shown recently, the insertion of *p*-phenylendiamine (PD) units into macrocyclic molecular backbones can lead to alleviation of the Coulombic penalty between charged triarylaminium radical centers in aza[1_n]metacyclophanes and to lower their oxidation potentials.[15]

On the other hand, tetraaza[1_4]*m*,*p*,*m*,*p*-cyclophane (**1**), the smallest macrocyclic oligoarylamine bearing the alternating *meta*–*para*-linkage, is known to create an almost pure spin-triplet diradical dication by two-electron oxidation.[16,17] In addition, we have shown that incorporation of the tetraazacyclophane moieties into a oligoarylamine backbone with one-

Received: December 19, 2012
Published: March 5, 2013

 © 2013 American Chemical Society

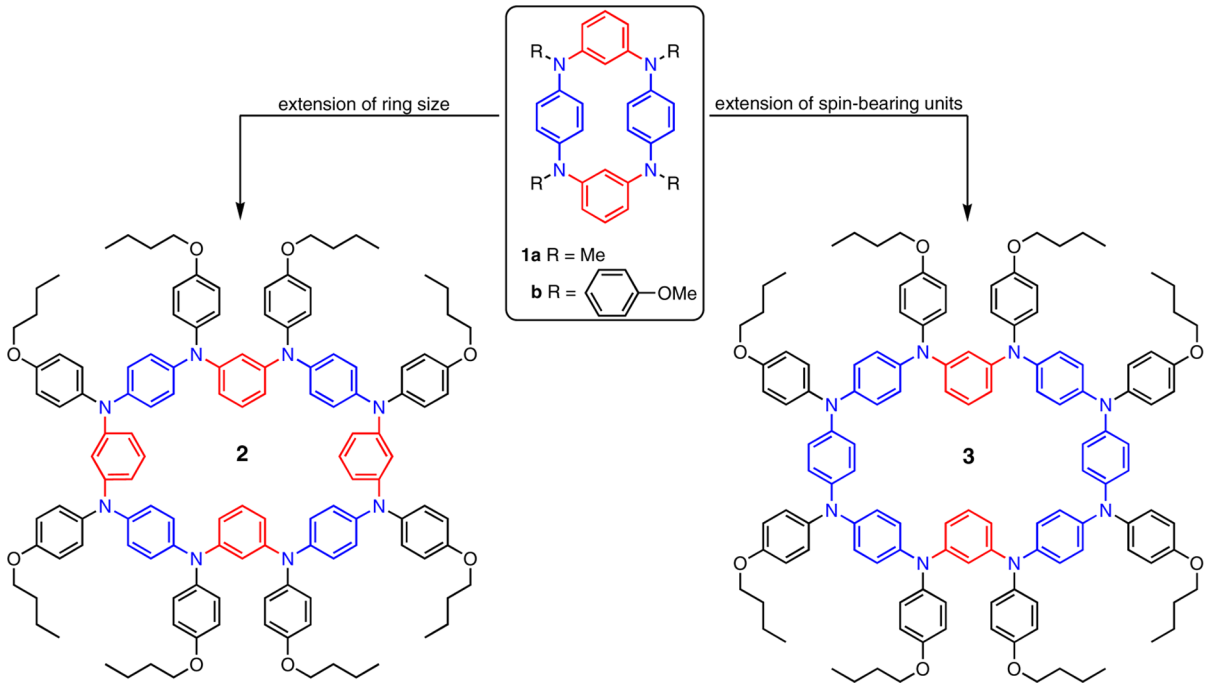

Figure 1. Two kinds of extension of tetraaza[1_4]*m,p,m,p*-cyclophane **1** and their target macrocycles **2** and **3**.

Scheme 1. Synthesis of Octaazacyclophanes 2 and 3

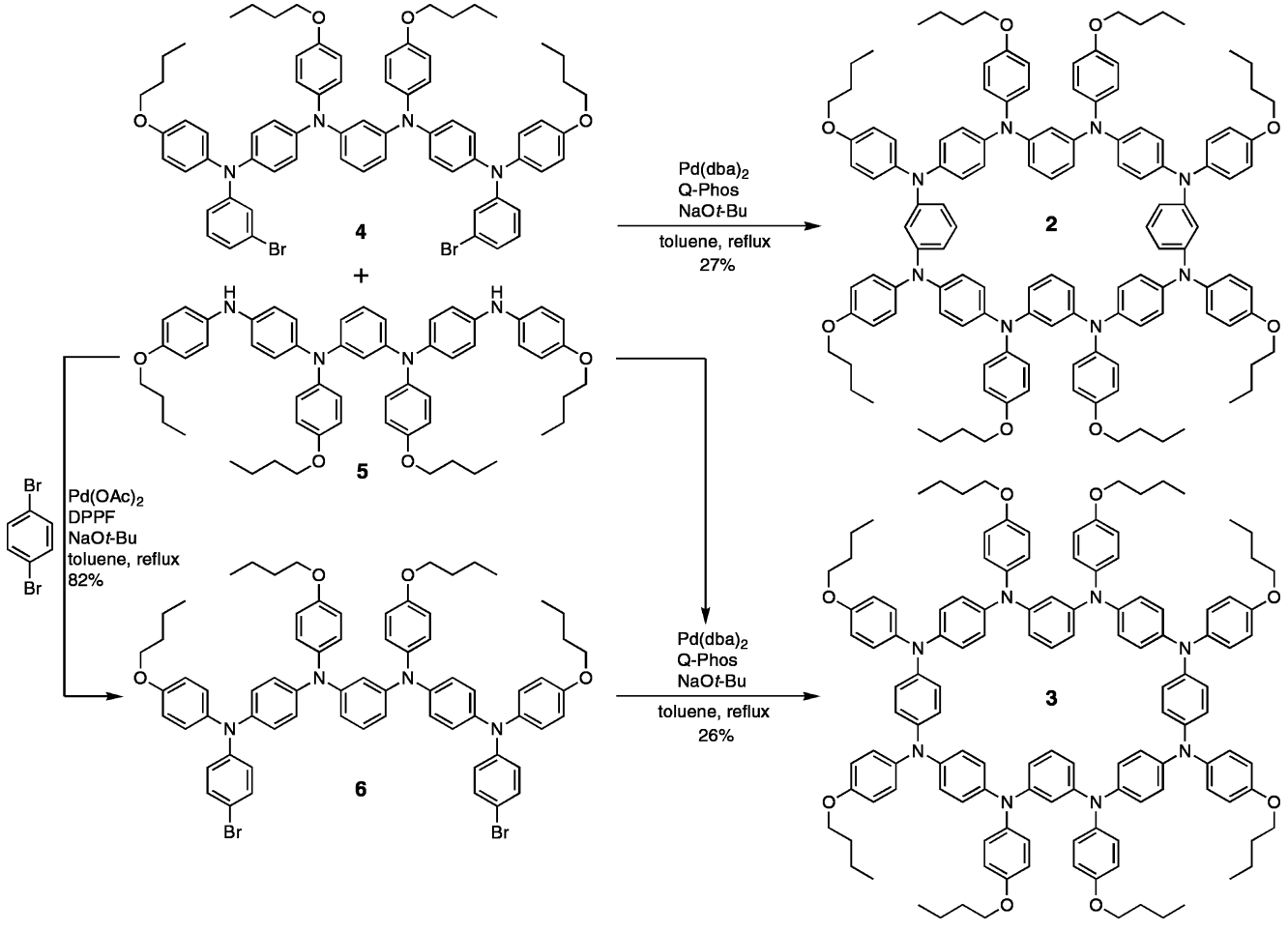

dimensional connectivity can overcome the inherent fragility in spin-coupling pathway of one-dimensional multispin systems and that the robust high-spin alignment in a one-dimensional multispin is recovered.[18] In this study, as extensions of **1**, we

dx.doi.org/10.1021/jo3026884 | J. Org. Chem. 2013, 78, 2947−2956

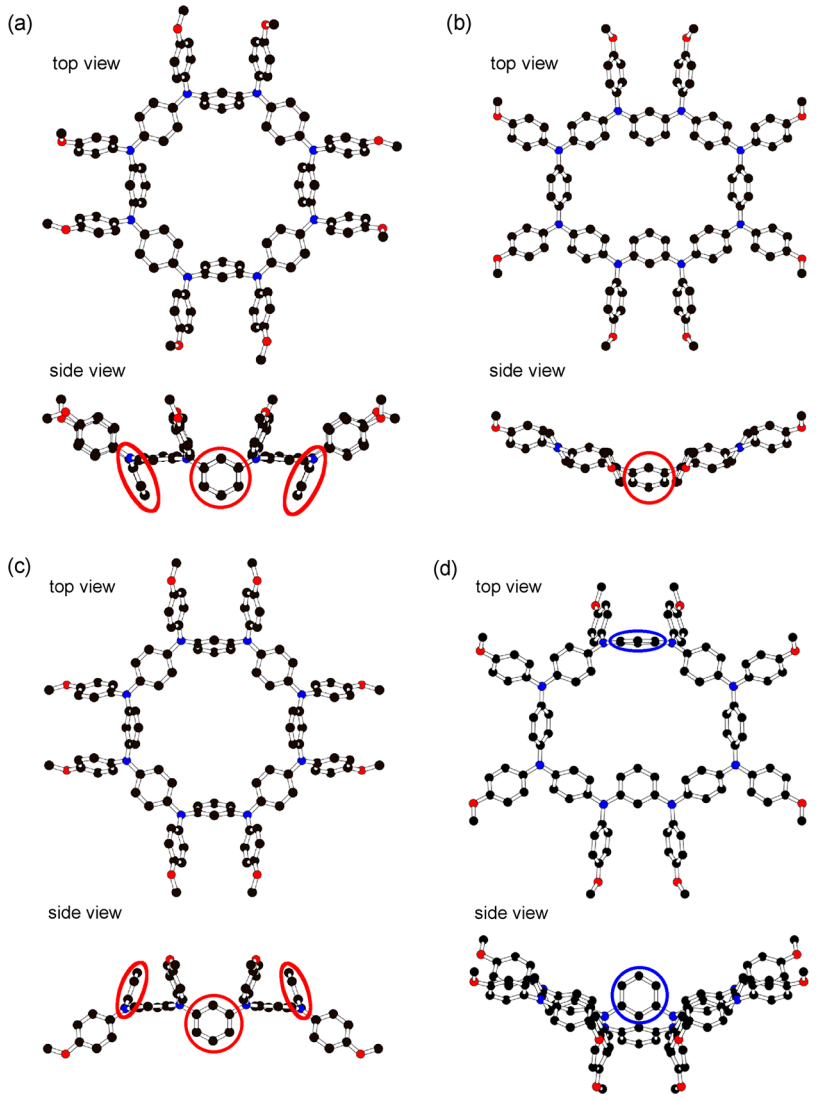

Figure 2. Optimized structures of the model compounds **2′** and **3′**: the lowest energy conformers for (a) **2′** (C_4) and (b) **3′** (C_{2v}), and the next lowest energy conformers for (c) **2′** (D_{2d}) and (d) **3′** (C_s). *m*-Phenylene rings in (a)−(c) are enclosed by red circles, and the flipped *m*-phenylene ring in (d) is enclosed by a blue circle.

prepared octaazacyclophanes with different linkage patterns: octaaza[1_8]*m*,*p*,*m*,*p*,*m*,*p*,*m*,*p*-cyclophane (**2**), which doubles the ring size of **1**, and octaaza[1_8]*m*,*p*,*p*,*p*,*m*,*p*,*p*,*p*-cyclophane (**3**), in which two extended *p*-phenylene-linked oligotriarylamines as spin-bearing units are linked by two *m*-phenylenes (Figure 1). Apparently, in the octaazacyclophane **2**, the structural rigidity can be weakened due to the extension of ring-size, and therefore, it is interesting to examine how such a flexible molecular structure influences the spin-coupling pathway in the polycationic species of **2**, as compared to that of $\mathbf{1}^{2+}$. In addition, the octaazacyclophane **3** enables us to judge whether the extended *p*-phenylene-linked oligotriarylamine moieties can serve as spin-containing units.[19]

RESULTS AND DISCUSSION

Synthesis. As shown in Scheme 1, *meta*−*para*-linked octaazacyclophanes **2** and **3** were prepared by the convergent fragment coupling approach[6] between tetraamine **5**[20] and the corresponding dihalides **4**[20] and **6** utilizing palladium-catalyzed aryl amination reaction (Buchwald−Hartwig reaction) as a key reaction. Although the generation of **2** by the same cross-coupling reaction of **5** with 1,3-dibromobenzene was also attempted, the main product was found to be tetraazacyclophane **1**, and we were unable to detect the desired product **2** in the reaction mixture.

Theoretical Considerations. To address the molecular[21] and electronic structures of **2** and **3**, we carried out the DFT calculations (B3LYP/6-31G*) on the model compounds **2′** and **3′**, in which all *n*-butoxy groups of **2** and **3** were replaced by methoxy groups to reduce the computational cost.[22] The global energy minimum of **2′** was predicted to be a pseudocone conformation (all of the *m*-phenylene rings are oriented in the same direction) with C_4 symmetry, while a pseudo-1,3-alternate conformer (all the adjacent *m*-phenylene rings are oriented in the opposite directions) with D_{2d} symmetry was estimated to be 0.89 kcal mol^{-1} less stable than the pseudocone conformer (Figure 2a and 2c).[23] Thus, all of the *m*-phenylene rings of **2** are anticipated to be inclined to the molecular plane defined by eight nitrogen atoms. On the other hand, a C_{2v}-symmetric conformer with a globally planar structure as compared to **2′** was placed at the global energy minimum for **3**, whereas the next lowest energy conformer (one of the *m*-phenylene rings is

dx.doi.org/10.1021/jo3026884 | J. Org. Chem. 2013, 78, 2947−2956

almost perpendicular to the slightly warped molecular plane) with C_s symmetry lay only 0.03 kcal mol^{-1} above the C_{2v} conformer (Figure 2b,d).[23] It should be noted that the popular B3LYP functional often leads to unsatisfactory results for molecular systems in which the medium-range interactions should be carefully treated. More importantly, Jorgensen and co-worker clarified that the average errors are about 3.0 kcal mol^{-1} for both isomerization energies and heats of formation of closed-shell organic compounds containing C, H, N, and O elements at the B3LYP/6-31G* level of theory.[24] This important clarification means that B3LYP calculations are nearly useless for energetic comparison between competing conformers in the present azacyclophanes. Hence, we have recalculated with the more reliable Minnesota density functional (M06-2X), which has improved performance for main-group thermochemistry, barrier heights, and noncovalent interactions as compared with the popular B3LYP functional.[25] As a consequence, the relative energies between two competing conformers were estimated to be 5.18 and 0.02 kcal mol^{-1} for **2′** and **3′**, respectively. In addition, the M06-2X-optimized geometries for two conformers were similar to the B3LYP-optimized geometries (Figure S6, Supporting Information). Although the trend remained unchanged for the M06-2X calculations, more elaborate quantum chemical methods may be necessary for more clear estimation of the relative energies. However, we can safely say that the presence of the energetically low-lying conformers predicts the flexible structures of **2** and **3**. This point was reflected in the observed variable-temperature ^{1}H NMR spectra of **2** and **3** (Figures S1 and S2, Supporting Information). The ^{1}H NMR spectra of **2** and **3** at room temperature showed simple signals due to the rapid interconversion between the competing conformers. Decreasing the temperature to 183 K caused broadening of all the signals, and some new signals appeared. However, the sharp signals corresponding to each conformer were not observed above 183 K, and thus, we could not get information on the coalescence temperature and the interconversion barriers. This result also supports the flexible structures of **2** and **3**.

The calculated frontier Kohn−Sham MOs of **2′** (HOMO, doubly degenerate (HO-1)MOs, and (HO-2)MO) are shown in Figure 3a. The energy gap between HOMO and (HO-2)MO was evaluated to be small (0.21 eV), and moreover, judging from their MO patterns, they can be classified as nondisjoint or coexistensive MOs.[7,26] Accordingly, when four electrons are removed from **2**, the resulting tetracation is predicted to be in a spin-quintet state. In the case of model compound **3′**, however, the energy gap between the (HO-1)MO and (HO-2)MO was relatively large, whereas the HOMO and (HO-1)MO were quasi-degenerate. As a consequence, it is anticipated that the higher oxidized states, $\mathbf{3}^{3+}$ and $\mathbf{3}^{4+}$, are in spin-doublet and closed-shell electronic structures, respectively, while dication $\mathbf{3}^{2+}$ is predicted to be in a spin-triplet state. Note that similar MO energy diagrams were obtained for the M06-2X/6-31G* calculations (Figure S7, Supporting Information).

Electrochemistry and Spectroelectrochemistry. In order to estimate the multielectron redox activity originating from four *p*-phenylenediamine (PD) units in **2** and two *p*-phenylene-linked oligotriarylamine units in **3**, we measured the cyclic voltammograms of **2** and **3** in CH_2Cl_2 containing 0.1 M *n*-Bu_4NBF_4 as the supporting electrolyte at 298 K. As shown in Figure 4, the redox behaviors of **2** and **3** are roughly viewed as four reversible oxidation steps (1e, 1e, 2e, and 4e for **2** and 2e, 2e, 1e, and 3e for **3**; *n*e = number of electrons). Differential pulse voltammetry (DPV) and the digital simulation[27] of the observed DPV curves afforded the oxidation potential at each oxidation process for **2** and **3** (Figure 5). The oxidation potentials of **2**, **3**, and the reference compounds [*N*,*N*,*N*′,*N*′-tetraanisyl-*p*-phenylenediamine (**TAPD**) and tetraazacyclophane **1b**] are summarized in Table 1. This result indicates that both of the present octaazacyclophanes are oxidizable up to their respective octacations, corresponding to the number of nitrogen atoms as redox-active centers. As compared to the large E_3-E_2 separation (0.32 V) for **1b**, the first four one-electron oxidation processes of **2** correspond to the formation of four semiquinoidal PD radical cations, while the remaining one two-electron oxidation and two one-electron oxidation processes give rise to the formation of four quinoidal PD dications, leading to a spinless state. On the other hand, the large E_3-E_2 separation (0.23 V) for **3** can be interpreted by the generation of the delocalized radical cation on each *p*-phenylene-linked oligotriarylamine units. More noteworthy is that the first oxidation potential (E_1 = −0.24 V) of **3** was

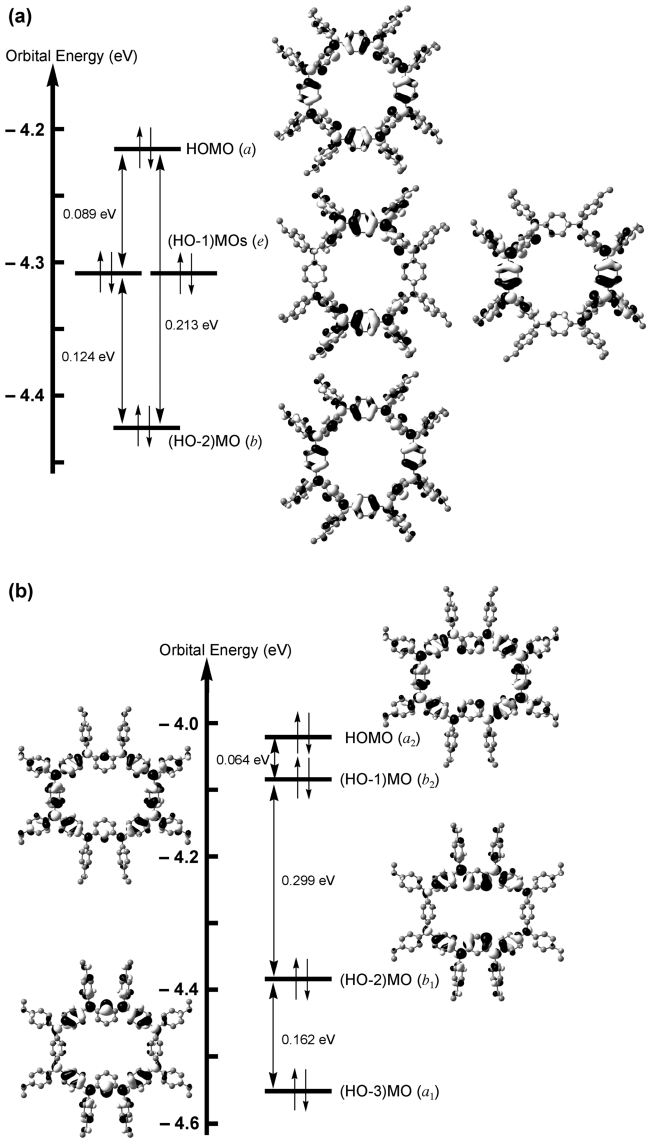

Figure 3. Relative energy levels of the frontier Kohn−Sham molecular orbitals for the model compounds (a) **2′** and (b) **3′** based on calculations at the B3LYP/6-31G* level.

dx.doi.org/10.1021/jo3026884 | J. Org. Chem. 2013, 78, 2947−2956

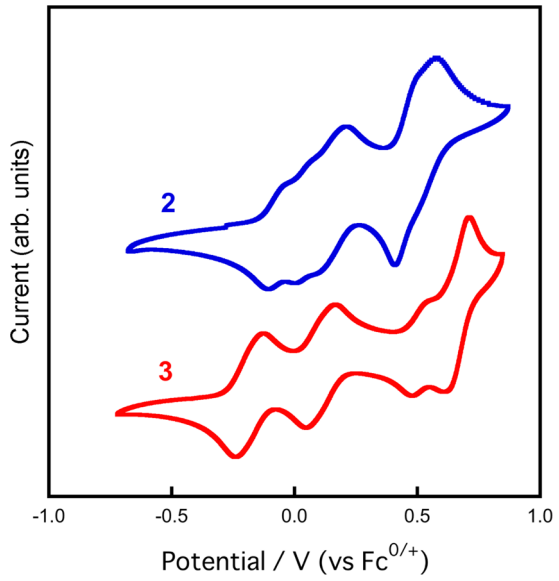

Figure 4. Cyclic voltammograms (CV) of **2** (blue curve) and **3** (red curve), measured in CH_2Cl_2 (at 1×10^{-3} M) containing 0.1 M *n*-Bu_4NBF_4 at 298 K (scan rate 100 mV s^{-1}).

considerably lower than those of **1b** (E_1 = −0.01 V) and **2** (E_1 = −0.09 V). This result indicates that the generated radical cation is stabilized by spin- and/or charge delocalization due to elongation of π-conjugation in the *p*-phenylene-linked oligotriarylamine unit. In addition, since the third and fourth oxidations of **3** also take place at the lower oxidation potentials (E_3 = +0.05 V; E_4 = +0.12 V), the formation of tetracation for **3** is strongly facilitated as compared with tetraazacyclophane **1b** (E_3 = +0.54 V; E_4 = +0.67 V).

To provide information on the electronic structure at each oxidation step of **2** and **3**, we have measured the UV−vis−NIR absorption spectral change during the course of the oxidation of **2** and **3** by using an optically transparent thin-layer electrochemical cell. The spectral changes during the oxidation process of **2** to $\mathbf{2}^{2+}$ are shown in Figure 6a. As the oxidation proceeds, a π−π* band at 3.90 eV (318 nm) for **2** was changed into three new bands corresponding to the oxidized states from $\mathbf{2}^{+}$ to $\mathbf{2}^{2+}$ [1.29 eV (960 nm), 2.16 eV (575 nm), and 3.01 eV (412 nm)] with an isosbestic point at 3.50 eV (354 nm). The lowest observed energy band can be regarded as the so-called charge-resonance (CR) Class III intervalence band (IV) band owing to the formation of the semiquinone radical cation of the *p*-phenylenediamine (PD) moiety[28−30] and showed a slight blue shift (1.25 ($\mathbf{2}^{+}$) to 1.29 eV ($\mathbf{2}^{2+}$)) with increasing oxidation number, as is often observed for oligoarylamines containing several PD moieties.[11,18,30−32] Upon oxidation from $\mathbf{2}^{2+}$ to $\mathbf{2}^{4+}$, three emerging bands exhibited continuous increase in absorbance with an isosbestic point at 3.37 eV (368 nm), and finally the absorbance reached up to twice that of $\mathbf{2}^{2+}$ (Figure 6b). As is shown in Figure 6c, it should be noted that the absorbance in lower-energy region of the CR Class III IV band of $\mathbf{2}^{2+}$ decreased during the course of the oxidation from $\mathbf{2}^{2+}$ to $\mathbf{2}^{4+}$ with an isosbestic point at 0.94 eV (1325 nm), clearly demonstrating the decrease of absorbance in the weak Class II intervalence charge-transfer (IVCT) band (which is often masked by the intense CR Class III IV and/or other bands)[18,33] between the neutral and one-electron oxidized PD moieties through *m*-phenylene linkers, accompanied by the disappearance of the charge-transferable neutral PD moieties. This indicates the coexistence of two types of the IV states, that is, the localized Class II and delocalized Class III states, in a single molecule, as is observed in organic IV compounds with multiple redox-active centers linked by both *m*-phenylene and *p*-phenylene linkers.[29] When $\mathbf{2}^{4+}$ was further oxidized, the intense CR Class III IV band began to decrease and a new band at 1.58 eV (786 nm) emerged with an isosbestic point at 1.45 eV (855 nm). This new band is attributable to the formation of diamagnetic dicationic quinoidal PD structures (Figure 6d).[34]

Turning now to the spectral change during the oxidation of neutral **3** to the dication, similar with that for **2**, three low energy bands at 0.97 eV (1272 nm), 2.34 eV (530 nm), and 2.79 eV (444 nm) continued to grow with a blue shift (ca. 0.85 ($\mathbf{3}^{+}$) to 0.97 eV ($\mathbf{3}^{2+}$)) of the lowest energy band (Figure 7a). The lowest energy band can be ascribed to be of charge-resonance type and is accompanied by two shoulders at 1.31 eV (950 nm) and 1.80 eV (690 nm), which are probably ascribed to partially resolved vibrational fine structure, as is typically observed in delocalized Class III IV compounds,[35,36] and therefore, it is strongly suggested that the generated charge and/or spin is delocalized over the *p*-phenylene-linked

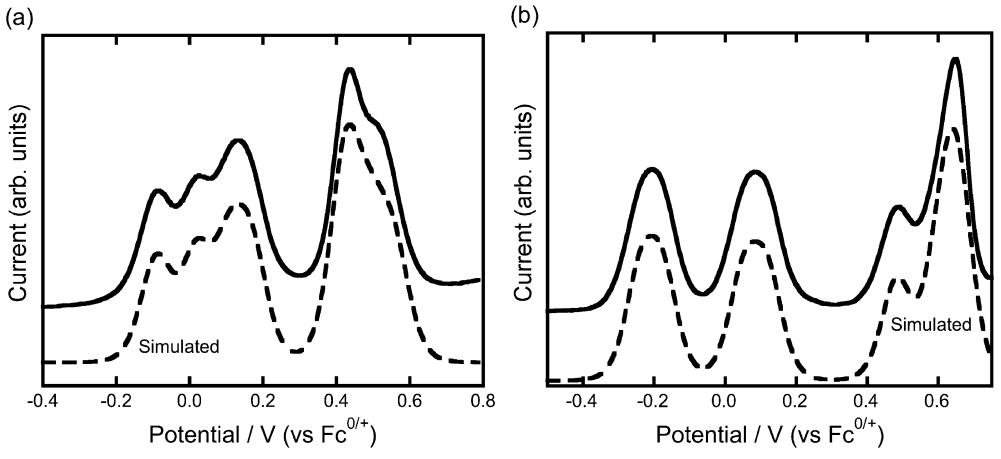

Figure 5. Differential pulse voltammograms (DPV) of (a) **2** and (b) **3**, measured in CH_2Cl_2 (at 1×10^{-3} M) containing 0.1 M *n*-Bu_4NBF_4 at 298 K (scan rate 100 mV s^{-1}). The simulated DPVs are drawn with a broken line, and the oxidation potentials listed in Table 1 were estimated by the digital simulation of the observed DPVs.

dx.doi.org/10.1021/jo3026884 | J. Org. Chem. 2013, 78, 2947−2956

Table 1. Oxidation Potentials (V versus $Fc^{0/+}$) by Cyclic Voltammetry and Differential Pulse Voltammetry (Scan Rate: 0.1 V s^{-1}) of 2, 3, and Related Compounds in CH_2Cl_2 (0.1 M n-Bu_4BF_4) at 298 K

compd	E_1	E_2	E_3	E_4	E_5	E_6	E_7
TAPD[a]	−0.13	+0.35					
1b[b]	−0.01	+0.22	+0.54	+0.67			
2[c]	−0.09	+0.02	+0.11	+0.17	+0.43[d]	+0.50	+0.56
3[c]	−0.24	−0.18	+0.05	+0.12	+0.48	+0.60	+0.65[d]

[a]Taken from ref 15. [b]Taken from ref 26. [c]Determined from the digital simulation of the observed DPV. [d]Quasi-two-electron transfer.

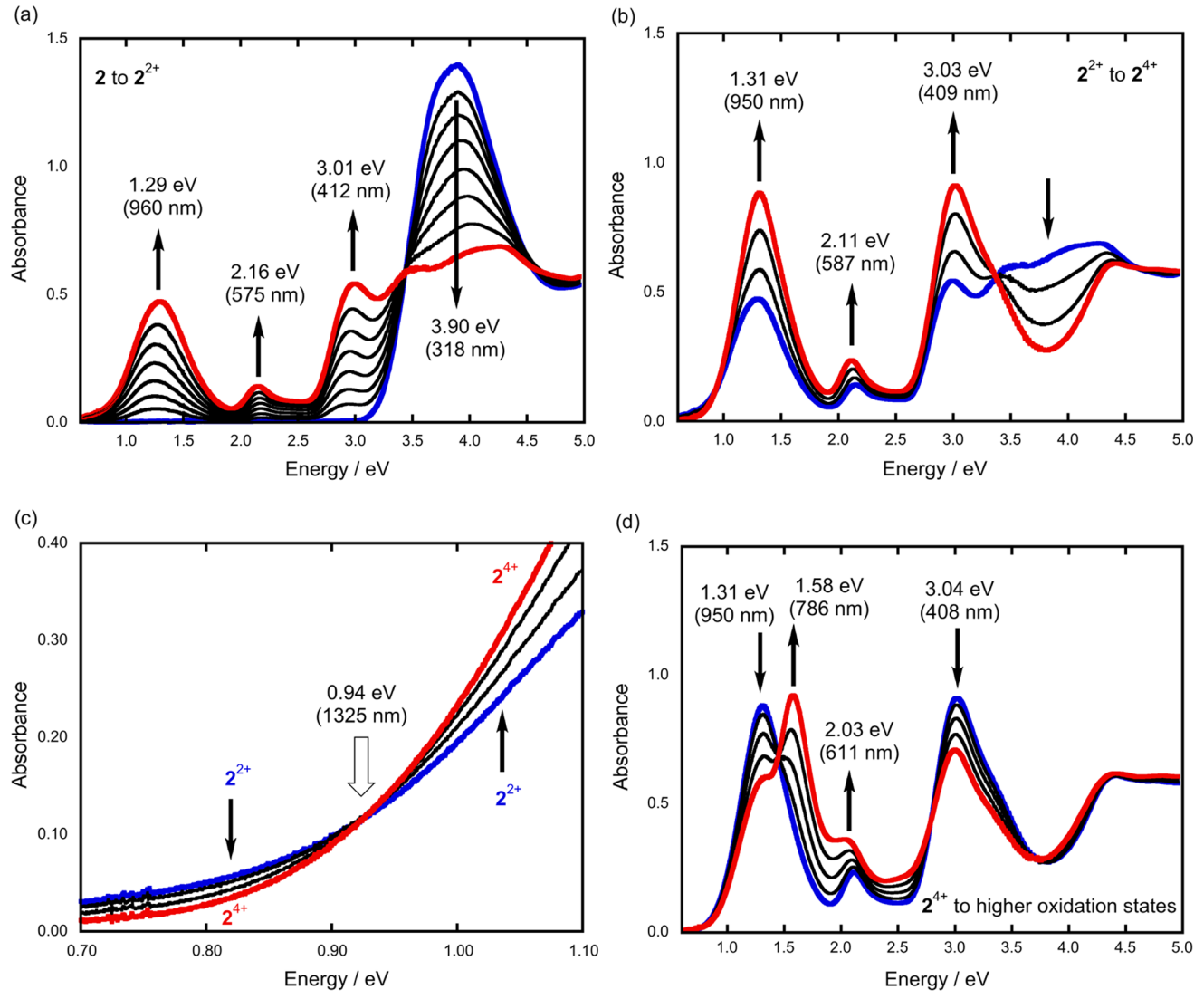

Figure 6. UV−vis−NIR absorption spectra of the stepwise electrochemical oxidation of **2** in CH_2Cl_2 (at 1×10^{-4} M) with 0.1 M n-Bu_4NBF_4 at 298 K: (a) **2** (in blue) to $\mathbf{2}^{2+}$ (in red); (b) $\mathbf{2}^{2+}$ (in blue) to $\mathbf{2}^{4+}$ (in red); (c) enlargement of the NIR region for the oxidation process from $\mathbf{2}^{2+}$ (in blue) to $\mathbf{2}^{4+}$ (in red); (d) further oxidation process from $\mathbf{2}^{4+}$ (in blue).

oligotriarylamine unit of **3**. Upon further oxidation from $\mathbf{3}^{2+}$ to $\mathbf{3}^{4+}$, both the blue shift (1.03 eV (1200 nm)) and the increase in the intensity of the lowest energy band were observed together with an isosbestic point around 0.90 eV (1385 nm) (Figure 7b). When the electrode potential exceeded the oxidation potential of $\mathbf{3}^{4+}$, this trend toward the blue shift and increase in intensity of the lowest energy band remained unchanged with appearance of a new isosbestic point around 0.99 eV (1250 nm) (Figure 7c). Accordingly, we could observe no definite spectral change corresponding to the structural change from the semiquinoidal structure to the quinoidal one of PD moieties, which was observed in the spectral change for **2** (Figure 6d). This is probably due to the constraints of the macrocyclic molecular structure, which hinders the planarization of molecular structure accompanied by the quinoidal deformation of PD moieties. Similar spectral changes are also seen for the dendritic all-*p*-phenylene-linked origoarylamines, in which the difficulty in quinoidal deformation of PD moieties is probably due to overcrowding by bulky dendron groups.[30]

ESR Spectroscopy. In order to estimate the effect by the extension of macrocyclic ring size from tetraazacyclophane **1** to octaazacyclophanes **2** and **3**, we examined the spin-multi-

dx.doi.org/10.1021/jo3026884 | J. Org. Chem. 2013, 78, 2947−2956

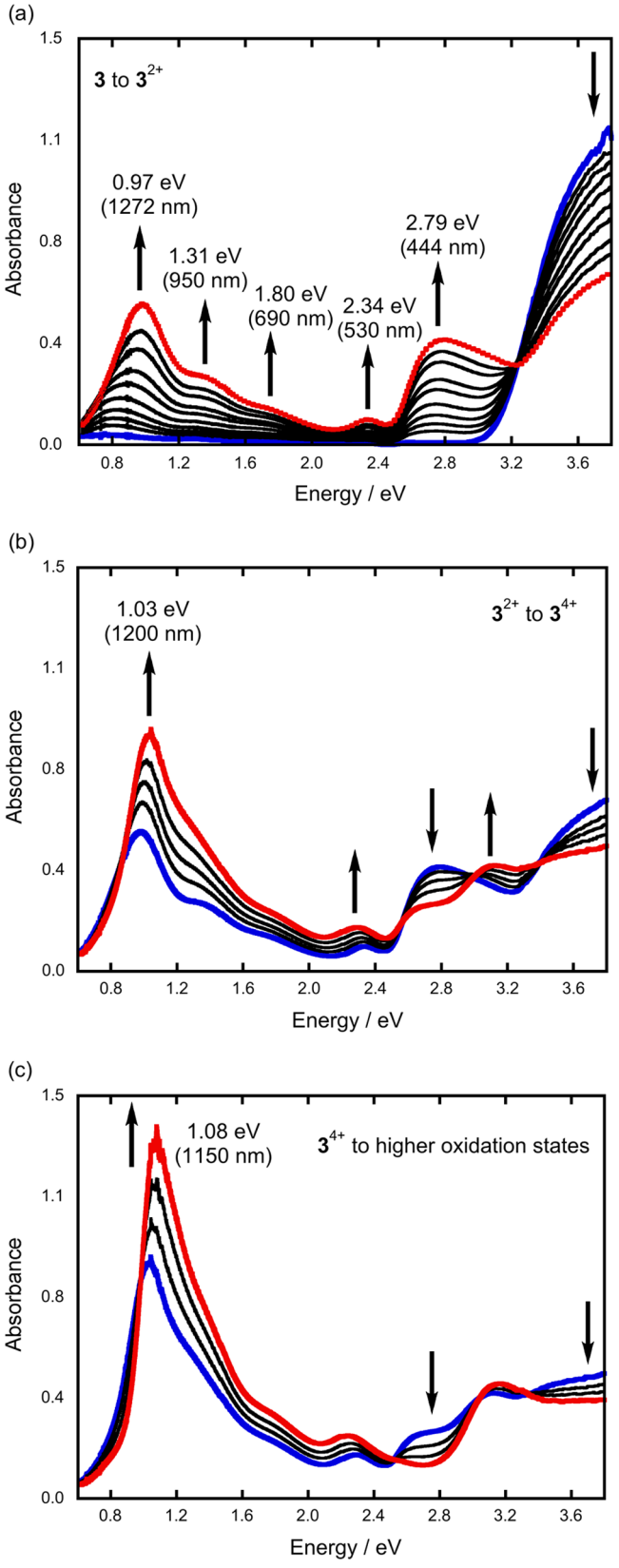

Figure 7. UV–vis–NIR absorption spectra of the stepwise electrochemical oxidation of **3** in CH_2Cl_2 (at 1×10^{-4} M) with 0.1 M *n*-Bu_4NBF_4 at 298 K: (a) **3** (in blue) to $\mathbf{3}^{2+}$ (in red); (b) $\mathbf{3}^{2+}$ (in blue) to $\mathbf{3}^{4+}$ (in red); (c) further oxidation process from $\mathbf{3}^{4+}$ (in blue).

plicities for the polycationic species of **2** and **3**. The present quantum chemical, electrochemical, and spectroelectrochemical studies on **2** and **3** open the possibility that the dicationic and tetracationic species for **2** and the dicationic species for **3** are accessible by appropriate chemical oxidations. The oxidized samples of **2** and **3** were generated at 195 K by adding 2 and/or 4 equiv of tris(4-bromophenyl)aminium hexachloroantimonate (Magic Blue).[37] To determine the spin multiplicity of the high-spin components of each oxidation state for **2** and **3**, we carried out the electron spin transient nutation (ESTN) measurements based on the pulsed ESR method.[38] The observed nutation frequency ω_{nut} for an allowed spin-state transition from $|S, M_S\rangle$ to $|S, M_S + 1\rangle$ can be approximately represented by the following relationship:

$$\omega_{nut} = \sqrt{S(S+1) - M_S(M_S+1)}\,\omega_0 \quad (1)$$

This equation indicates that ω_{nut} can be scaled with the total spin quantum number S and the spin magnetic quantum number M_S in a unit of ω_0, which corresponds to the nutation frequency for the spin–doublet species ($\omega_{doublet}$). The field-swept ESTN spectra observed for each oxidation state for **2** and **3** are shown in Figure 8. The projection along the magnetic field axis approximately corresponds to the usual continuous wave ESR (CW-ESR) spectrum, while the projection along the frequency axis corresponds to the transient nutation spectrum. The nutation frequencies observed for each oxidation state of **2** and **3** are summarized in Table 2. As shown in Figure 8a, the ESTN spectrum showed two signals corresponding to the spin-doublet and spin-triplet states, when **2** was treated with 2 molar equiv of oxidant. Apparently, the signal intensity of the spin-doublet state was larger than that of the spin-triplet state. The two unpaired spins generated are probably localized on opposite sides of the macrocyclic structure so as to reduce the Coulombic repulsion interactions. As a consequence, the magnetic interaction between two unpaired spins was strongly attenuated due to the resulting long spin-coupling pathway. When oxidized with 4 molar equiv of oxidant, the oxidized species exhibited four nutation signals corresponding to different spin states (S = 1/2, 1, 3/2, and 2) (Figure 8b). The spin-quintet signals (26.0 and 31.0 MHz) indicate that four unpaired spins localized on four PD units are ferromagnetically coupled through *m*-phenylene ferromagnetic coupler in the macrocyclic structure, as is also predicted from quasi-degenerate nondisjoint MOs (Figure 3a). However, the definite competing spin-triplet signal (19.4 MHz) reveals that the spin triplet-quintet energy splitting is considerably smaller, probably due to attenuation of spin-coupling pathway by facile conformational change. In addition, the spin-quartet species originating from partially oxidized $\mathbf{2}^{3+}$ were not negligible. This finding suggests that the present ring extension to alternating *meta-para*-linked octaazacyclophane **2** attenuates the spin-coupling pathway, and in this regard, octaazacyclophane **2** is similar to linear oligoarylamines.[39]

In contrast, the ESTN spectrum for dication $\mathbf{3}^{2+}$ generated by treatment with 2 molar equiv of oxidant clearly displayed the formation of an almost pure spin-triplet state (Figure 8c). On the other hand, when **3** was treated with 4 molar equiv of oxidant, the ESTN signal almost disappeared and only a very weak spin-doublet signal was observed, thus indicating the generated $\mathbf{3}^{4+}$ is diamagnetic, although the corresponding absorption spectrum showed no bands ascribed to the quinoidal structure of *p*-phenylene-linked oligotriarylamine unit of **3** (Figure 7). This result is also supported by

dx.doi.org/10.1021/jo3026884 | J. Org. Chem. 2013, 78, 2947–2956

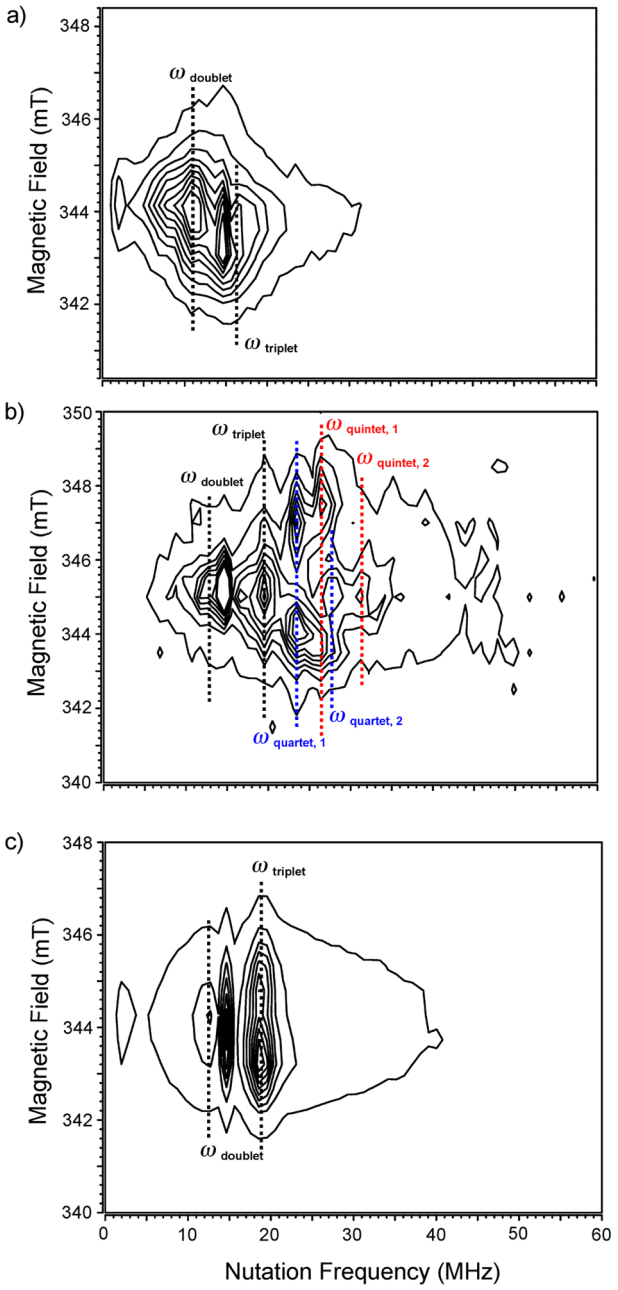

Figure 8. Magnetic field-swept electron-spin transient nutation (ESTN) spectra of **2** (after the addition of (a) 2 and (b) 4 molar equiv of Magic Blue) and **3** (after the addition of (c) 2 molar equiv of Magic Blue) in CH_2Cl_2 at 5 K. The intense signal observed at ca. 14 MHz is due to the electron spin echo envelope modulation (ESEEM),[40] which results from weak interaction with proton nuclei (I = 1/2) originating from the solvent molecules surrounding the paramagnetic species.

comparison of the CW-ESR spectra between $\mathbf{3}^{2+}$ and $\mathbf{3}^{4+}$ (Figure S8, Supporting Information).

CONCLUSION

The alternate *meta*–*para*-linked octaazacyclophane **2** and the macrocycle **3** containing extended *p*-phenylene-linked oligoarylamine moieties as spin-bearing units were prepared as simple extensions of tetraaza[1_4]*m*,*p*,*m*,*p*-cyclophane (**1**). The DFT calculations on the model compounds suggested that such an expansion of the macrocyclic ring-size leads to facile conformational changes and that both macrocycles are categorized into nondisjoint or coextensive molecules, which serve as promising candidates for high-spin molecules. From the electrochemical measurements, both macrocycles exhibited multiredox activity, and thus, they are oxidizable up to the octacation. Owing to the different linkage patterns, however, there are clear differences in the electronic structures of both macrocycles: (i) the UV–vis-NIR spectroelectrochemical measurements revealed that the generated charges and/or unpaired spins are mainly confined into *p*-phenylenediamine (PD) moieties in **2**, thus allowing the deformation from the semiquinoidal to the quinoidal structure with increasing oxidation number, whereas higher oxidation states for **3** did not show definite quinoidal deformation of PD moieties, (ii) Pulsed ESR measurements demonstrated that almost pure spin-triplet state was realized for $\mathbf{3}^{2+}$, whereas unpaired spins in $\mathbf{2}^{2+}$ and $\mathbf{2}^{4+}$ were virtually uncoupled even at low temperatures, probably due to fragility of spin-coupling pathway caused by facile conformational changes. In addition, $\mathbf{3}^{4+}$ was found to be a closed-shell electronic structure. Overall, as has been already pointed out for linear oligoarylamines, conformational flexibility resulted in the fragility in spin-coupling pathway for multispin systems, even in **2**. On the other hand, it was suggested that the extension of spin-bearing units does not affect the high-spin correlation of macrocyclic multispin systems, as has been exemplified by the diradical dications of **3**.

EXPERIMENTAL SECTION

Materials. Commercial grade reagents were purchased and used without further purification procedures. Solvents were purified, dried, and degassed by following standard procedures. Compounds **4** and **5** were synthesized according to literature procedures, and were checked by ^{1}H NMR, ^{13}C NMR, and FAB LRMS spectroscopy.

Preparation of Compound 6. A mixture of **5** (0.59 g, 0.67 mmol), *p*-dibromobenzene (1.91 g, 8.10 mmol), $Pd(OAc)_2$ (0.076 g, 0.03 mmol), 1,1′-bis(diphenylphosphanyl)ferrocene (DPPF) (0.039 g, 0.07 mmol), and NaO-*t*-Bu (0.268 g, 2.79 mmol) in toluene (3.4 mL) was refluxed under an argon atmosphere for 36 h. After evaporation of the solvent, the residue was dissolved in CH_2Cl_2 and washed with brine. The organic layer was separated and dried over Na_2SO_4. After evaporation of the solvent, the crude product was chromatographed on silica gel (toluene/hexane = 1:1 as eluent) to afford **6** (0.66 2g, 82.8%) as a pale yellow solid: mp 99–100 °C; ^{1}H NMR (400 MHz, acetone-d_6) δ = 0.939–0.986 (m, 12H), 1.432–1.543 (m, 8H), 1.693–1.780 (m, 8H), 3.929–3.981 (m, 8H), 6.432 (dd, J = 2.20, 8.05 Hz, 2H), 6.682 (t, J = 2.20 Hz, 1H), 6.802–7.046 (m, 29H), 7.307 (d, J = 9.03 Hz, 4H); ^{13}C NMR (100 MHz, acetone-d_6) δ = 14.2, 20.0, 32.2, 68.6, 103.2, 115.3, 115.7, 116.3, 116.5, 123.3, 125.3, 125.9, 128.1, 128.3, 130.5, 132.8, 140.8, 141.0, 142.9, 144.2, 148.8, 149.9, 157.0, 157.31; HR-ESI-MS m/z calcd for $C_{70}H_{72}N_4O_4Br_2$ 1190.3915, found 1190.3933 $[M]^+$.

Preparation of Compound 2. Anhydrous toluene (100 mL) was added to $Pd(dba)_2$ (0.016 g, 0.027 mmol), $Ph_5FcP(t\text{-}Bu)_3$ (Q-Phos)[41] (0.037 g, 0.052 mmol), and NaO-*t*-Bu (0.196 g, 2.036 mmol) in a flask equipped with a dropping funnel which was charged with a toluene solution (50 mL) of **4** (0.443 g, 0.501 mmol) and **5** (0.599 g, 0.502 mmol), and the toluene solution was stirred under an argon atmosphere at 110 °C for a while. The solution in the dropping funnel was gradually added to the solution containing the palladium catalyst for 1 h, and then the reaction mixture was refluxed for 21 h with stirring. The reaction mixture was cooled to room temperature, washed with brine, and dried over Na_2SO_4. After evaporation of the solvent, the crude product was chromatographed on silica gel (toluene/hexane = 2:1 as eluent) to afford **2** (0.259 g, 26.9%) as a white powder: mp 271–272 °C; ^{1}H NMR (400 MHz, tetrahydrofuran-d_8) δ = 0.964 (t, J = 7.32 Hz, 24H), 1.485 (m, 16H), ~1.7 (m,16H; the corresponding signals are masked by the solvent signal (due to the

dx.doi.org/10.1021/jo3026884 | J. Org. Chem. 2013, 78, 2947–2956

Table 2. Spectroscopic Data of the ESTN Spectroscopy for Poly(radical cation)s of 2 and 3

species	obsd mutation frequency (MHz)	transition assignment
2^{2+}	16.8 ($\omega_{triplet} = \sqrt{2}\ \omega_{doublet}$)	|1, ± 1> ⇔ |1, 0>
(doublet impurity)	11.5 ($\omega_{doublet}$)	|1/2,+1/2> ⇔ |1/2, −1/2>)
2^{4+}	26.0 ($\omega_{quartet,\ 1} = 2\omega_{doublet}$)	|2, ± 2> ⇔ |2, ± 1>
	31.0 ($\omega_{quartet,\ 2} = \sqrt{6}\ \omega_{doublet}$)	|2, ± 1> ⇔ |2, 0>
(quartet impurity)	23.4 ($\omega_{quartet,\ 1} = \sqrt{3}\ \omega_{doublet}$)	|3/2,± 3/2> ⇔ |3/2, ± 1/2>
	27.4 ($\omega_{quartet,\ 2} = 2\ \omega_{doublet}$)	|3/2,+1/2> ⇔ |3/2, −1/2>)
(competing triplet)	19.4 ($\omega_{triplet} = \sqrt{2}\ \omega_{doublet}$)	|1, ± 1> ⇔ |1, 0>)
(doublet impurity)	13.0 ($\omega_{doublet}$)	|1/2,+1/2> ⇔ |1/2, −1/2>)
3^{2+}	18.3 ($\omega_{triplet} = \sqrt{2}\ \omega_{doublet}$)	|1, ± 1> ⇔ |1, 0>
(doublet impurity)	13.0 ($\omega_{doublet}$)	|1/2,+1/2> ⇔ |1/2, −1/2>)

β-protons)), 3.882 (t, J = 6.34 Hz, 16H), 6.360 (dd, J = 2.20, 8.29 Hz, 8H), 6.757 (d, J = 9.03 Hz, 16H), 6.846 (m, 24H), 6.964 (d, J = 9.03 Hz, 16H); ^{13}C NMR (100 MHz, tetrahydrofuran-d_8) δ = 14.2, 20.2, 32.4, 68.3, 115.2, 115.8, 124.6, 127.7, 141.0, 143.1, 149.7, 156.6; HR-ESI-MS m/z calcd for $C_{128}H_{136}N_8O_8$ 1913.0476, found 1913.0539 $[M]^+$. Anal. Calcd for $C_{128}H_{136}N_8O_8$: C, 80.30; H, 7.16; N, 5.85; O, 6.69. Found: C, 80.50; H, 7.27; N, 5.87; O, 6.92.

Preparation of Compound 3. Anhydrous toluene (100 mL) was added to $Pd(dba)_2$ (0.013 g, 0.023 mmol), $Ph_5FcP(t\text{-}Bu)$[3] (Q-Phos)[34] (0.0029 g, 0.040 mmol), and NaO-*t*-Bu (0.155 g, 1.610 mmol) in a flask equipped with a dropping funnel, which was charged with a toluene solution (50 mL) of **5** (0.351 g, 0.397 mmol) and **6** (0.471 g, 0.394 mmol), and the toluene solution was stirred under an argon atmosphere at 110 °C for a while. The solution in the dropping funnel was gradually added to the solution containing the palladium catalyst, and then the reaction mixture continued stirring. After 16 h, the reaction mixture was refluxed for 20 h. The reaction mixture was cooled to room temperature, washed with brine, and dried over Na_2SO_4. After evaporation of the solvent, the crude product was chromatographed on silica gel (toluene as eluent) to afford **3** (0.197 g, 26.0%) as a pale yellow powder: mp 156−157 °C; ^{1}H NMR (400 MHz, tetrahydrofuran-d_8) δ = 0.963 (t, J = 7.56 Hz, 24H), 1.487 (m, 16H), ∼1.7 (m, 16H; the corresponding signals are masked by the solvent signal (due to the β-protons)), 3.834 (m, 16H), 6.295 (dd, J = 1.95, 8.05 Hz, 4H), 6.734 (d, J = 8.78 Hz, 8H), 6.785−6.880 (m, 36H), 6.941 (d, J = 9.03 Hz, 8H), 7.018 (d, J = 8.78 Hz, 8H); ^{13}C NMR (100 MHz, tetrahydrofuran-d_8): δ = 14.18, 14.20, 20.1, 20.2, 32.4, 32.5, 68.4, 68.4, 114.3, 115.9, 115.9, 124.0, 124.9, 125.5, 126.9, 128.0, 128.9, 129.6, 141.1, 141.7, 142.8, 143.5, 144.2, 149.7, 156.3, 156.9; HR-ESI-MS m/z calcd for $C_{128}H_{136}N_8O_8$ 1913.0476, found 1913.0544 $[M]^+$. Anal. Calcd for $C_{128}H_{136}N_8O_8$: C, 80.30; H, 7.16; N, 5.85; O, 6.69. Found: C, 80.42; H, 7.15; N, 5.70; O, 6.82.

■ ASSOCIATED CONTENT

Supporting Information

General experimental methods, ^{1}H and ^{13}C NMR spectra of all new compounds, computational details and optimized geometries for **2′** and **3′**, electrochemical and spectroelectrochemical measurements, and ESR and pulsed ESR measurements. This material is available free of charge via the Internet at http://pubs.acs.org.

■ AUTHOR INFORMATION

Corresponding Author

*E-mail: aito@scl.kyoto-u.ac.jp.

Present Address

[⊥]Center for Instrumental Analysis, Institute for Research Promotion, Niigata University, 8050, Ikarashi 2-no-cho, Nishiku, Niigata 950-2181, Japan.

Notes

The authors declare no competing financial interest.

■ ACKNOWLEDGMENTS

This work was supported by a Grant-in-Aid for Scientific Research (B) (24310090) from the Japan Society for the Promotion of Science (JSPS). D.S. thanks the JSPS Research Fellowship for Young Scientists.

■ REFERENCES

(1) (a) König, B.; Fonseca, M. H. *Eur. J. Inorg. Chem.* **2000**, 2303. (b) Wang, M.-X. *Chem. Commun.* **2008**, 4541. (c) Maes, W.; Dehaen, W. *Chem. Soc. Rev.* **2008**, *37*, 2393. (d) Takemura, H. *Curr. Org. Chem.* **2009**, *13*, 1633. (e) Wang, M.-X. *Acc. Chem. Res.* **2012**, *45*, 182. (f) Cragg, P. J.; Sharma, K. *Chem. Soc. Rev.* **2012**, *41*, 597.

(2) (a) Chen, P.; Jäkle, F. *J. Am. Chem. Soc.* **2011**, *133*, 20142. (b) Chen, P.; Lalancette, R. A.; Jäkle, F. *Angew. Chem., Int. Ed.* **2012**, *51*, 7994.

(3) Tsue, H.; Ishibashi, K.; Tamura, R. *Top. Heterocycl. Chem.* **2008**, *17*, 73.

(4) Ito, A.; Tanaka, K. *Pure Appl. Chem.* **2010**, *82*, 979.

(5) (a) Ito, A.; Ono, Y.; Tanaka, K. *New J. Chem.* **1998**, 779. (b) Ito, A.; Ono, Y.; Tanaka, K. *J. Org. Chem.* **1999**, *64*, 8236.

(6) (a) Wang, M.-X.; Zhang, X.-H.; Zheng, Q.-Y. *Angew. Chem., Int. Ed.* **2004**, *43*, 838. (b) Wang, M.-X.; Yang, H.-B. *J. Am. Chem. Soc.* **2004**, *126*, 15412. (c) Liu, S.-Q.; Wang, D.-X.; Zheng, Q.-Y.; Wang, M.-X. *Chem. Commun.* **2007**, 3856. (d) Zhang, E.-X.; Wang, D.-X.; Zheng, Q.-Y.; Wang, M.-X. *Org. Lett.* **2008**, *10*, 2565.

(7) Bushby, R. J.; Kilner, C. A.; Taylor, N.; Vale, M. E. *Tetrahedron* **2007**, *63*, 11458.

(8) Ishibashi, K.; Tsue, H.; Sakai, N.; Tokita, S.; Matsui, K.; Yamauchi, J.; Tamura, R. *Chem. Commun.* **2008**, 2812.

(9) Vale, M.; Pink, M.; Rajca, S.; Rajca, A. *J. Org. Chem.* **2008**, *73*, 27.

(10) Panagopoulos, A. M.; Zeller, M.; Becker, D. P. *J. Org. Chem.* **2010**, *75*, 7887.

(11) Ito, A.; Yokoyama, Y.; Aihara, R.; Fukui, K.; Eguchi, S.; Shizu, K.; Sato, T.; Tanaka, K. *Angew. Chem., Int. Ed.* **2010**, *49*, 8205.

(12) Tsuchiya, K.; Miyaishi, H.; Ogino, K. *Chem. Lett.* **2011**, *40*, 931.

(13) (a) Wolfe, J. P.; Wagaw, S.; Marcoux, J. F.; Buchwald, S. L. *Acc. Chem. Res.* **1998**, *31*, 805. (b) Hartwig, J. F. *Acc. Chem. Res.* **1998**, *31*, 852. (c) Hartwig, J. F. *Angew. Chem., Int. Ed.* **1998**, *37*, 2046. (d) Muci, A. R.; Buchwald, S. L. *Top. Curr. Chem.* **2002**, *219*, 133.

(14) (a) Bushby, R. J.; McGill, D. R.; Ng, K. M.; Taylor, N. *Chem. Commun.* **1996**, 2641. (b) Bushby, R. J.; McGill, D. R.; Ng, K. M.; Taylor, N. *J. Chem. Soc., Perkin Trans. 2* **1997**, 1405.

(15) Ito, A.; Inoue, S.; Hirao, Y.; Furukawa, K.; Kato, T.; Tanaka, K. *Chem. Commun.* **2008**, 3242.

(16) (a) Ito, A.; Ono, Y.; Tanaka, K. *Angew. Chem., Int. Ed.* **2000**, *39*, 1072. (b) Selby, T. D.; Blackstock, S. C. *Org. Lett.* **1999**, *1*, 2053. (c) Hauck, S. I.; Lakshmi, K. V.; Hartwig, J. F. *Org. Lett.* **1999**, *1*, 2057.

(17) Kulszewicz-Bajer, I.; Maurel, V.; Gambarelli, S.; Wielgus, I.; Djurado, D. *Phys. Chem. Chem. Phys.* **2009**, *11*, 1362.

(18) Sakamaki, D.; Ito, A.; Furukawa, K.; Kato, T.; Tanaka, K. *Chem. Commun.* **2009**, 4524.

(19) Hexaaza[1_6]*m,p,p,m,p,p*-cyclophane with a similar linkage pattern to macrocycle **3** was reported in ref 17.

(20) Goodson, F. E.; Hauck, S. I.; Hartwig, J. F. *J. Am. Chem. Soc.* **1999**, *121*, 7527.
(21) Despite several trials, we failed to obtain single crystals of **2** and **3** suitable for the X-ray structural analysis.
(22) To check the influence of optimized macrocyclic structures in **2** and **3** by replacing long *n*-butoxy groups with short methoxy groups, we carried out semiempirical AM1 (Austin model 1 calculations on both **2**, **2′**, **3**, and **3′**. Dewar, M. J. S.; Zoebisch, E. G.; Healy, E. F.; Stewart, J. J. P. *J. Am. Chem. Soc.* **1985**, *107*, 3902. As shown in Figures S3 and S4 in the Supporting Information, the replacement of long alkyl chains with short ones did not affect the optimized structures. Thus, we conducted the DFT calculations of the model compounds **2′** and **3′** with methoxy groups.
(23) Prior to the DFT calculations on the most and the next stable conformers of **2′** and **3′**, we performed the semiempirical AM1 calculations on possible conformers of **2′** and **3′**. For **2′**, four conformers are possible depending on the orientations of four *meta*-phenylene rings: all four rings are upward to the molecular plane (C_4 confomer); the four rings are alternately upward and downward to the molecular plane (D_{2d} conformer); one ring is solely downward to the molecular plane (C_s conformer); and the adjacent two rings are upward and the others are downward to the molecular plane (C_{2h} conformer) (Figure S5, Supporting Information). As a consequence, the relative energies for C_4, D_{2d}, C_s, and C_{2h} conformers were predicted to be 0.0, 0.99, 1.18, and 1.27 kcal mol^{-1}, respectively, as compared to the C_4 conformer. In contrast, in the AM1 optimizations on **3′**, it was found that the C_{2v}- and C_s-symmetric conformations were promising candidates (Figure S4(a) and (c), Supporting Information. Contrary to the DFT results, however, the C_{2v} conformer lay 0.31 kcal mol^{-1} above the C_s conformer.
(24) Tirado-Rives, J.; Jorgensen, W. L. *J. Chem. Theory Comput.* **2008**, *4*, 297.
(25) (a) Zhao, Y.; Truhlar, D. G. J. *Chem. Phys.* **2006**, *125*, 194101. (b) Zhao, Y.; Truhlar, D. G. *Acc. Chem. Res.* **2008**, *41*, 157. (c) Zhao, Y.; Truhlar, D. G. *Chem. Phys. Lett.* **2011**, *502*, 1.
(26) (a) Borden, W. T.; Davidson, E. R. *J. Am. Chem. Soc.* **1977**, *99*, 4587. (b) Dougherty, D. A. *Acc. Chem. Res.* **1991**, *24*, 88.
(27) Huang, W.; Henderson, T. L. E.; Bond, A. M.; Oldham, K. B. *Anal. Chim. Acta* **1995**, *304*, 1.
(28) (a) Ishitani, A.; Nagakura, S. *Mol. Phys.* **1967**, *12*, 1. (b) Badger, B.; Brocklehurst, B.; Russell, R. D. *Chem. Phys. Lett.* **1967**, *1*, 122. (c) Szeghalmi, A. V.; Erdmann, M.; Engel, V.; Schmitt, M.; Amthor, S.; Kriegisch, V.; Nöll, G.; Stahl, R.; Lambert, C.; Leusser, D.; Stalke, D.; Zabel, M.; Popp, J. *J. Am. Chem. Soc.* **2004**, *126*, 7834.
(29) Hirao, Y.; Ito, A.; Tanaka, K. *J. Phys. Chem. A* **2007**, *111*, 2951.
(30) Ito, A.; Sakamaki, D.; Ichikawa, Y.; Tanaka, K. *Chem. Mater.* **2011**, *23*, 841.
(31) Ito, A.; Yamagishi, Y.; Fukui, K.; Inoue, S.; Hirao, Y.; Furukawa, K.; Kato, T.; Tanaka, K. *Chem. Commun.* **2008**, 6573.
(32) Sakamaki, D.; Ito, A.; Furukawa, K.; Kato, T.; Shiro, M.; Tanaka, K. *Angew. Chem., Int. Ed.* **2012**, *51*, 12776.
(33) (a) Bonvoisin, J.; Launay, J.-P.; Van der Auweraer, M.; De Schryver, F. C. *J. Phys. Chem.* **1994**, *98*, 5052. Correction: Bonvoisin, J.; Launay, J.-P.; Van der Auweraer, M.; De Schryver, F. C. *J. Phys. Chem.* **1996**, *100*, 18006. (b) Bonvoisin, J.; Launay, J.-P.; Verbouwe, W.; Van der Auweraer, M.; De Schryver, F. C. *J. Phys. Chem.* **1996**, *100*, 17079. (c) Sedó, J.; Ruiz, D.; Vidal-Gancedo, J.; Rovira, C.; Bonvoisin, J.; Launay, J.-P.; Veciana, J. *Adv. Mater.* **1996**, *8*, 748. (d) Wienk, M. M.; Janssen, R. A. J. *J. Am. Chem. Soc.* **1997**, *119*, 4492. (e) Rovira, C.; Ruiz-Molina, D.; Elsner, O.; Vidal-Gancedo, J.; Bonvoisin, J.; Launay, J.-P.; Veciana, J. *Chem.—Eur. J.* **2001**, *7*, 240.
(34) The absorption band attributable to the formation of dicationic quinoidal PD structures for *N*,*N*,*N*′,*N*′-tetraanisyl-*p*-phenlenediamine (TAPD) is observed at 769 nm (1.61 eV): Lambert, C.; Nöll, G. *J. Am. Chem. Soc.* **1999**, *121*, 8434.
(35) Nelsen, S. F.; Konradsson, A. E.; Weaver, M. N.; Telo, J. P. *J. Am. Chem. Soc.* **2003**, *125*, 12493.
(36) Ito, A.; Nakano, Y.; Urabe, M.; Kato, T.; Tanaka, K. *J. Am. Chem. Soc.* **2006**, *128*, 2948.
(37) (a) Bell, F. A.; Ledwith, A.; Sherrington, D. C. *J. Chem. Soc.* **1969**, 2719. (b) Connell, N. G.; Geiger, W. E. *Chem. Rev.* **1996**, *96*, 877.
(38) (a) Isoya, J.; Kanda, H.; Norris, J. R.; Tang, J.; Brown, M. K. *Phys. Rev. B* **1990**, *41*, 3905. (b) Astashkin, A. V.; Schweiger, A. *Chem. Phys. Lett.* **1990**, *174*, 595.
(39) Ito, A.; Sakamaki, D.; Ino, H.; Taniguchi, A.; Hirao, Y.; Tanaka, K.; Kanemoto, K.; Kato, T. *Eur. J. Org. Chem.* **2009**, 4441.
(40) Mims, W. B. *Phys. Rev. B* **1972**, *5*, 2409.
(41) (a) Shelby, Q.; Kataoka, N.; Mann, G.; Hartwig, J. *J. Am. Chem. Soc.* **2000**, *122*, 10718. (b) Kataoka, N.; Shelby, Q.; Stambuli, J. P.; Hartwig, J. F. *J. Org. Chem.* **2002**, *67*, 5553.